Climate change, age acceleration, and the erosion of fitness in polar bears

Authors: Levi Newediuk[1], Evan S Richardson[1,2,*], Brooke A. Biddlecombe[1], Haziqa Kassim[3], Leah Kathan[1], Nicholas Lunn[2], L Ruth Rivkin[1,4,5], Ola E Salama[3], Chloé Schmidt[6], Meaghan J Jones[3,*], Colin J Garroway[1,*]

Affiliations:
[1] Department of Biological Sciences, University of Manitoba, Canada
[2] Environment and Climate Change Canada
[3] Department of Biochemistry and Medical Genetics, University of Manitoba, and Children's Hospital Research Institute of Manitoba, Canada
[4] Polar Bears International, Bozeman, MT, USA
[5] San Diego Zoo Wildlife Alliance, Escondido, California, USA
[6] German Centre for Integrative Biodiversity Research (iDiv) Halle-Jena-Leipzig, Leipzig, Germany

Corresponding authors: Levi Newediuk (Levi.Newediuk@umanitoba.ca), Meaghan J Jones (Meaghan.Jones@umanitoba.ca), Evan S Richardson (Evan.Richardson@ec.gc.ca), Colin J Garroway (Colin.Garroway@umanitoba.ca)
* Denotes co-PIs

Abstract

Rapid climate change is expected to impose strong selective pressures on wild populations, disrupting evolved life history strategies and limiting population viability[1]. The magnitude and pace at which environments will change means the persistence of wild populations will depend substantially on their ability to adapt genetically. However, we know very little about the capacity for evolutionary change in response to the rapid pace and predicted magnitude of warming. The Arctic is the fastest warming region on the planet[2], so that is where we can first address this knowledge gap. Using estimates of epigenetic age acceleration, which indicate the accumulation of stress exposures across lifetimes[3,4], we found polar bears (*Ursus maritimus*) in western Hudson Bay, Canada aged one year faster on average for each degree Celsius of temperature rise they experienced. As predicted by established theory, age acceleration was associated with reproducing early, a trait that prior to the onset of rapid warming, increased lifetime reproductive success for bears. However, the fitness benefit of early reproduction eroded with increased warming, reflecting a redirection of energy away from reproduction toward maintenance. Finally, we found no evidence for recent selection on traits associated with lifetime reproductive success. It appears that the fitness costs of increased lifetime stressful exposures associated with warming leaves little scope for genetic adaptation in this population. These findings, together with global forecasts of abrupt exposure of species to intolerable temperature extremes[5], warn that adaptive responses to warming could be the exception rather than the rule.

Main

Climate change is causing extreme environmental fluctuations and persistent warming, exposing species to conditions increasingly distant from those they evolved to tolerate[6]. Species have typically responded to environmental change through range shifts[7], changes in seasonally timed behaviours[8], and population declines[9]. However, the accumulation of our past emissions and current emission targets commit the planet to ongoing warming for the foreseeable future[10]. This means that the persistence of many species will ultimately rely on their capacity to adapt genetically to the rapidly changing environment. Maintaining a population's adaptive potential is a central tenet of conservation biology. However, the extent to which populations can respond evolutionarily to the rapid pace of climate warming is poorly understood. Using modern biomedical techniques, we tested for increases in epigenetic age, which represents the accumulation of lifetime stressful exposures at the cellular level, associated with exposure to four decades of warming in an intensively studied polar bear (*Ursus maritimus*) population in western Hudson Bay, Canada. We then linked epigenetic age acceleration in individuals to the erosion of fitness and adaptive potential at the population level (Figure 1). The Arctic has warmed at a rate approximately four times greater than the global mean and is now 3°C warmer, on average, than it was at the onset of rapid warming[2]. If current emission targets are met, the rest of the planet will warm by ~3°C by the end of the century[11]. Our results offer a window into whether we might expect widespread adaptive change by wildlife populations to levels of warming that will be reached globally in the near future.

The western Hudson Bay polar bear population is at the southern edge of the Arctic and has been subject to standardized annual sampling and individual-based monitoring since 1980 (Figure 1). Polar bears rely on sea ice for travel and mating and as a platform to hunt their

62 primary prey, ringed (*Pusa hispida*) and bearded (*Erignathus barbatus*) seals. After sea ice
63 retreats in spring, prey become inaccessible, and polar bears must fast, relying on accumulated
64 fat reserves for growth, reproduction, and survival[12]. As a result of air and sea surface
65 temperature anomalies associated with this warming[13], the ice-free season in the Hudson Bay
66 region has lengthened by approximately ten days per decade since the early 1980s[14,15]. During
67 this time the population size has declined by nearly 50% to its current estimated abundance of
68 just over 600 individuals[16]. Sea ice loss is firmly tied to population decline and is the most
69 significant climate-related threat to this population [14,15,17–19]. Longer ice-free seasons increase the
70 bears' fasting period on land, and each additional day of fasting requires metabolizing
71 approximately one kilogram of body mass[20]. Bears also risk losing stored body mass as thinning
72 winter ice and rapid spring melts force longer swims between ice floes. Swimming is five times
73 more energetically expensive for bears than walking, and dramatically longer swims are required
74 for even small changes in sea ice[21].

75 **Increase in age acceleration with climate warming**

76 In 1956, Hans Selye observed that 'Every stress leaves an indelible scar, and the organism pays
77 for its survival after a stressful situation by becoming a little older'[22]. Biomedical research has
78 since established that an organism's cumulative experience of stressful environmental conditions
79 is reflected in its cellular aging rate, or its biological age. When cells age faster, organisms
80 become biologically older than their chronological age would suggest, a phenomenon called
81 biological age acceleration[23,24]. Importantly, age acceleration reflects the cumulative experiences
82 of an individual, both good and bad, across lifetimes[24]. We measured biological age acceleration
83 in western Hudson Bay polar bears using an epigenetic approach recently developed in
84 biomedicine[4,25,26].

Epigenetic age is measured through DNA methylation, a process in which methyl groups are attached to DNA molecules at cytosine guanine dinucleotides or CpG sites[23]. This process plays a role in cell fate and gene regulation[27]. DNA methylation patterns at some CpG sites change so predictably across lifespans that they can be used to build "epigenetic clocks" for predicting chronological age in humans[28], mouse models[29], and many other mammals[30–35]. Epigenetic clocks predict chronological age two- to three-fold more accurately than earlier biological aging approaches such as telomere shortening[36]. Epigenetic age acceleration, estimated using the residual difference between chronological and predicted biological age[28], is currently the most accurate biomedical measure of cumulative experiences with environmental stressors and all-cause mortality in humans[4,37]. Critical for our purposes, epigenetic age acceleration can be estimated from archived tissue sampled from individuals with known chronological ages, both of which are available for this population. This methodological advance provided a lens with which we could view changes in the lifetime accumulation of lifetime stress in polar bears sampled across 40 years, starting before the onset of significant climate warming through to the recent period of rapid warming.

We built an epigenetic clock for polar bears with archived tissue samples. Our clock (Supplemental Data File 1) is based on blood and skin tissue DNA methylation rates from 144 male and female individuals aged 0–30 sampled between 1988–2016 (Supplemental Data File 2). We used elastic net regression and epigenome-wide association surveys to identify 125 CpG sites in the polar bear genome where DNA methylation is strongly associated with chronological age but unrelated to sex (Extended Data Figure 1). We narrowed these sites down from an initial 33,674 candidate CpG sites on the mammalian DNA methylation array[38] that align to the polar bear genome (Supplemental Data File 3). Our clock accurately tracked epigenetic age over the

lifetimes of bears with repeat samples (Figure 2 A-E) and predicted the chronological ages of an independent sample of 134 test bears within a median absolute error of 2.07 years (Figure 2 F), or approximately 5% of the maximum polar bear lifespan[39]. This performance is on par with the most accurate epigenetic clocks built for humans and other wildlife[28,31,32]. We used our epigenetic clock to estimate epigenetic age acceleration through time for the 134 test bears not used for clock development.

We found a clear signal of faster epigenetic aging with time that paralleled climatic warming and lengthening ice-free periods (Table 1; Figure 3). This suggests that the accumulation of their experiences with environmental stressors is causing increasing cellular aging through time. A causal role of reduced sea ice in age acceleration is supported by a spike in epigenetic age acceleration in 1990 (Figure 3). This spike coincides with one of the earliest spring melts on record in western Hudson Bay and one of the largest observed declines in polar bear survival[31]. Age accelerated at similar rates for males and females. On average, bears born in the 2010s were biologically 2.6 years older than bears born in the 1960s (Figure 3). Considering a 30-year lifespan, near the maximum for this population[40], a 2.6-year increase in epigenetic age is equivalent to an 8.7% increase in aging rate. Because of our sampling approach, however, this increase is likely a conservative estimate. We evenly selected samples from individuals across age classes, but polar bear survival rates decline significantly as they approach their early 20s[40]. Age acceleration is associated with increased morbidity and mortality[4,37], so the 20–30-year-old bears available to sample were likely among the healthiest of their cohort. This suggests we oversampled healthy bears and underestimated age acceleration.

129 **Evolutionary change and adaptive potential**

130 The costs of reproduction have important evolutionary repercussions[41,42]. Individuals take energy
131 and nutrients from the environment and allocate them to growth, self-maintenance, and
132 reproduction. Resources devoted to one area are unavailable for the others, meaning the optimal
133 allocation of energy to self-maintenance and reproduction depends on ecological setting[42].
134 Reproduction is particularly expensive, so reproducing early in life should come at the expense
135 of self-maintenance and longevity[41]. We observed a weak correlation between age acceleration
136 and age at first reproduction for 100 western Hudson Bay polar bears with estimates of both age
137 acceleration and age at first reproduction ($R^2_m = 0.12$; Table 1; Extended Data Figure 2). When
138 environments are variable and survival is uncertain, reproduction late in life is also uncertain, so
139 theory predicts selection for investing energy in reproducing earlier in life[41]. We could estimate
140 lifetime reproductive success, a common measure of fitness, for 628 individuals from the long-
141 term study. We found that in the 1980s, early reproducing bears had the highest lifetime
142 reproductive success (Table 1). However, the fitness advantage of reproducing early in life
143 declined through the 1990s. By 2000, bears produced the same number of offspring over their
144 lifetimes regardless of how young they were when they first reproduced (Figure 4 A). Increased
145 lifetime stress associated with climate warming appears to have reduced fitness by directing
146 energy toward self-maintenance and survival and away from reproduction.

147 All credible climate forecasts project ongoing warming for the foreseeable future. This
148 means that population persistence will depend on a population's overall capacity to adapt
149 genetically to the changing environment. We used our estimates of lifetime reproductive success
150 and a population pedigree that spanned the 40 year study[43] to estimate adaptive potential (i.e., the
151 contribution of selection to genetically-based increases in population mean fitness). Adaptive

potential is estimated as the additive genetic variance in individual relative fitness, which can be thought of as an estimate of the overall effect of selection on the ability of individuals to reproduce[44]. Fitting an animal model[45] with the 4,634-individual pedigree (923 dams, 443 sires), we found the additive genetic variance underlying lifetime reproductive success in this population was approximately zero (V_A(w) = 0.006; Extended Data Table 1). This suggests selection on traits related to individual fitness is not contributing to adaptive change. This lack of adaptation is consistent with its reduced survival and negative growth rates observed in the population through time[16], which are expected for populations experiencing substantial environmental change with limited capacity to respond adaptively[46]. Without gene flow from differently adapted populations or changes in selective regimes, this population has minimal adaptive capacity to cope with the ongoing long-term environmental change associated with climate warming.

Conclusions

The harmful effects of rapidly warming Arctic environments appear to be defying adaptive evolution in western Hudson Bay polar bears. Increases in the accumulation of lifetime stress, as indicated by accelerated aging, were associated with climate warming. To our knowledge, this is the first evidence of increased rates of biological aging in a wild population as a result of climate change. Faster aging is linked to deteriorating metabolic and physiological processes related to intracellular maintenance[3]. This deterioration should eventually entail reduced fitness, as we also observed. Age acceleration reflects an individual's cumulative lifetime experiences with its environment[4]. While the progression of climate warming is clear, there are good and bad years and thus good and bad environmental experiences, and age acceleration captures both[24]. Regardless of interannual variation, however, the net consequence of warming for polar bears

175 across their lifetimes is negative. The accumulation of lifetime stress as environments change
176 appears to be a general mechanism by which individual experiences with harsh environments can
177 scale up to reduce population mean fitness and cause demographic declines. With increasing
178 exposure to harsh environments, declines in abundance, and little evidence for adaptive capacity,
179 the Western Hudson Bay polar bear population faces a highly uncertain future.

180 The erosion of fitness and lack of adaptive potential in polar bears is instructive for
181 understanding whether other populations might respond adaptively to environmental change in
182 the coming decades. Warming in the Arctic has abruptly altered the ecosystem, and this
183 abruptness outpaced adaptive potential for polar bears. Recent modelling suggests that similarly
184 abrupt exposure to intolerable temperatures across large portions of species ranges could be
185 widespread in the coming decades[47]. At the current rate of warming, more than 30% of species
186 could be exposed to temperatures beyond those they evolved to tolerate by 2100[47,48]. As species
187 pass their thermal thresholds, the capacity for populations and ecosystems to adapt will diminish.
188 With the recent signing of the United Nations Montreal-Kunming Global Biodiversity
189 Framework, monitoring and conserving adaptive potential has become mandated in international
190 policy. This is a major positive step toward safeguarding biodiversity given ongoing climate
191 change and other threats. However, our results and the forecasts for future species exposure to
192 warming[47,48] warn that adaptive responses to warming could be the exception rather than the
193 rule. Significant conservation effort on all fronts and concerted effort to halt warming will be
194 necessary to safeguard biodiversity for future generations.

195 **Acknowledgments**

196 This work was supported by funding from Environment and Climate Change Canada and an
197 NSERC Discovery Grant awarded to CJG. We thank C. Kucheravy, E. Karachaliou, E. de Greef,

J. Suurväli, and C. Müller of the Population Ecology & Evolutionary Genetics Group at the University of Manitoba for comments on the manuscript. We also thank Q. Fletcher for helpful discussions while preparing the manuscript.

Table 1. Four decades of warming is linked to epigenetic aging and fitness declines in an intensively studied polar bear (*Ursus maritimus*) population in western Hudson Bay, Canada. Bears born more recently and those that reproduce earlier in life age faster epigenetically. The fitness benefit of earlier reproduction, estimated using lifetime reproductive success, declined for later-born bears. We report the fixed effect covariates and their coefficients from Bayesian generalized linear models testing relationships between epigenetic age acceleration, year of birth, age at first reproduction, and lifetime reproductive success for male and female polar bears. Probability of direction (P direction) describes the probability that a coefficient is either positive or negative, expressed as a percentage between 50% and 100%. Marginal R^2 (R^2_m) describes the proportion of variation in the response explained by the fixed effects relative to random effects, and conditional R^2 (R^2_c) describes the variation explained by fixed effects and random effects if included in the model. For all models, we used consevative weakly informative priors with mean = 0 and standard deviation = 1. We fit all models using the *brms* package v2.20.4 in R v4.3.1, with 4 chains and 10,000 iterations including 5,000 warmup iterations. Posterior predictive checks are in Extended Data Figure 3.

Variable	Covariates	Coefficient (95% CrI)	R^2m	R^2c	P direction
Age acceleration[§] (n = 134)	Year of birth	0.18 (-0.04, 0.40)	0.07	0.36	94.74
	Sex (M)	0.28 (-0.15, 0.71)			90.22
Age acceleration[§] (n = 100)	Age at first reproduction	-0.33 (-0.61, -0.03)	0.12	0.31	98.48
	Sex (M)	0.60 (0.07, 1.10)	-	-	98.48
Lifetime reproductive success[†] (n = 628)	Age at first reproduction	-0.16 (-0.22, -0.10)	-	0.15	100.00
	Year of birth	-0.34 (-0.43, -0.25)	-	-	100.00
	Sex (M)	-0.10 (-0.20, 0.01)		-	96.19
	Age at first reproduction: Year of birth	0.18 (0.08, 0.27)		-	100.00

[†]Models were specified using a negative binomial response distribution with a log link function.

[§]Models were specified using a Gaussian link function.

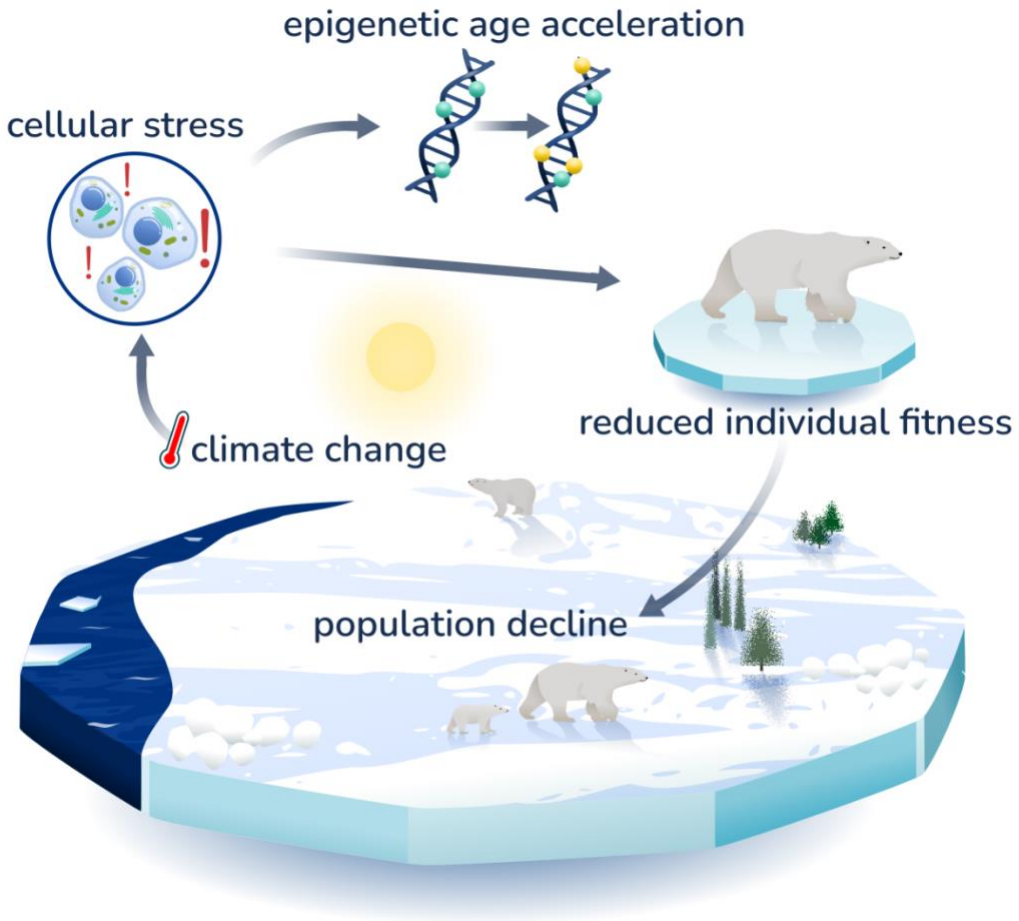

Figure 1. Epigenetic age acceleration predicts polar bear (*Ursus maritimus*) population declines caused by climate change. Global concerns over declining polar bear populations prompted formation of an international agreement on polar bear populations in the mid 1960s. Annual sampling and individual-based monitoring were standard in the western Hudson Bay subpopulation by 1980. Epigenetic aging rates accelerated over time with climate change (n = 134). Estimates of reproductive success for bears born between 1980 and 2000 (n = 628) suggest individual fitness has declined over time, coinciding with the erosion of advantages conferred by once-adaptive traits (n = 628) and a lack of adaptive capacity (n = 4,634). We linked declines in individual fitness to epigenetic age acceleration (n = 100).

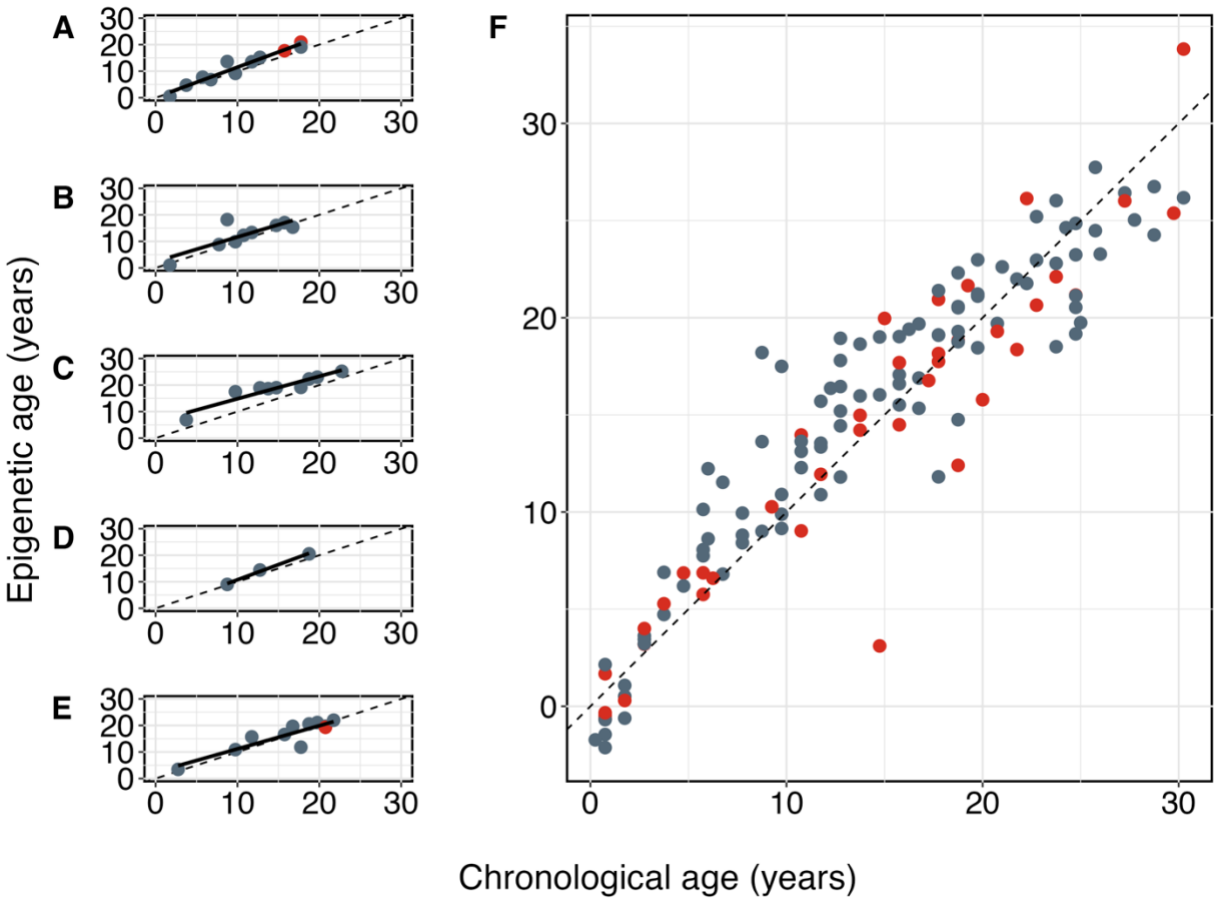

Figure 2. Our epigenetic clock for western Hudson Bay polar bears (*Ursus maritimus*) tracks aging over individual lifetimes (a–e) and accurately predicts chronological age within a median absolute error of 2.07 years for n = 134 bears (f). Epigenetic clocks estimate age using patterns of methylation at cytosine guanine dinucleotides on DNA molecules. We built our clock with archived blood and skin tissue samples from 144 male and female individuals aged 0–30 sampled between 1988–2016. Red points represent blood samples and grey points represent skin. The dotted line is a guide for a 1:1 relationship between chronological and epigenetic age. Points above this line indicate age acceleration, or individuals or samples that are epigenetically older than their chronological age.

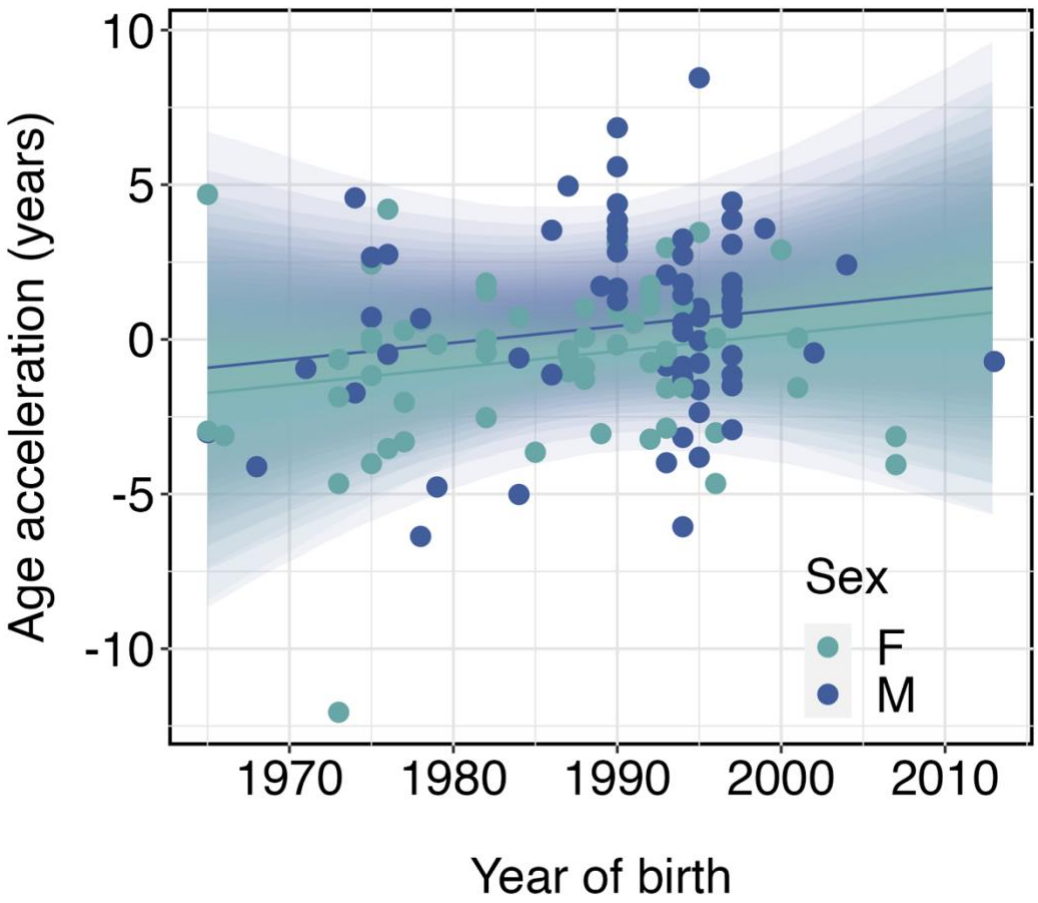

Figure 3. Epigenetic age acceleration, a cumulative measure of lifetime stressful exposures, has increased for both male (blue) and female (seafoam) polar bears (*Ursus maritimus*) in western Hudson Bay, Canada since annual monitoring began in the 1980s. Points represent measurements of epigenetic age acceleration from individuals born as early as 1965 and sampled between 1988 and 2016. The line and ribbon represent the mean and 95% credible interval around the posterior distributions estimated using a Bayesian generalized linear model.

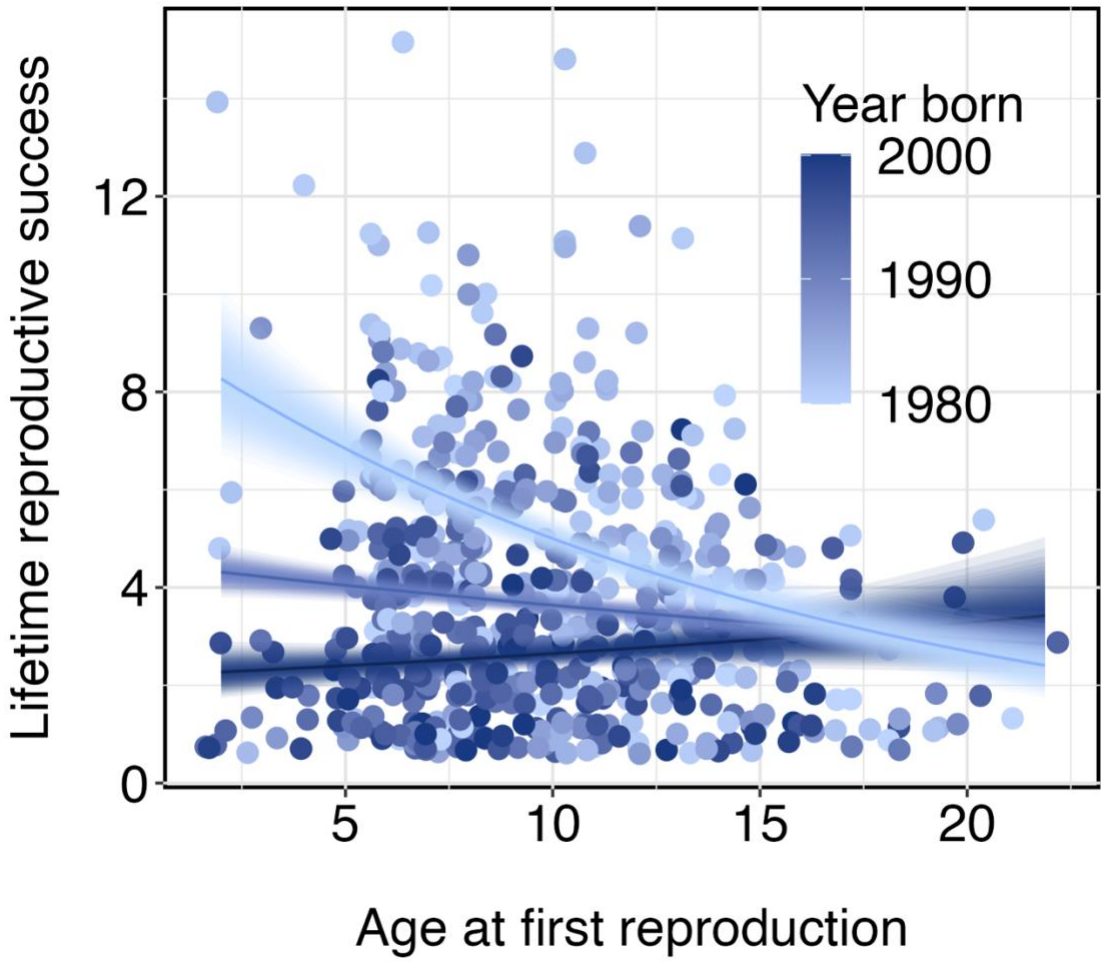

Figure 4. The fitness benefit of reproducing at younger ages eroded over two decades of climate change for n = 628 western Hudson Bay polar bears (*Ursus maritimus*). Reproducing at younger ages redirects energy from survival and self-maintenance, but theory predicts it can provide a fitness advantage in environments where reproduction is uncertain. In the 1980s when annual sampling began in this population, reproducing at younger ages increased fitness, which we estimated using lifetime reproductive success (light blue). Lifetime reproductive success declined for younger reproducers through the 1990s to 2000, at which point the fitness benefit of younger reproduction was lost (gradient from light to dark blue). Points show individual bear observations and lines are the predicted means of the posterior distributions in 1980, 1990, and 2000. Blue ribbons are 95% credible intervals.

Extended Data Table 1. Phenotypic mean and estimated random-effect sizes of lifetime reproductive success for Western Hudson Bay polar bears born between 1980 and 2000 using a univariate animal model with a 4,634-individual pedigree documented between 1966 and 2019 in northeastern Manitoba near Churchill, Canada. N_{ind} indicates the number of individuals with an estimate of observed lifetime reproductive success, a measure of relative fitness. V_P is the total phenotypic variance and is the sum of the variance components. Variance components are V_A=additive genetic 'animal', V_M=maternal 'dam' (i.e., identity of individual's dam), V_{YBirth}=cohort 'year of birth', and V_R=residual 'units'.Values in parentheses represent standard deviations (SD) or standard errors (SE).

Trait	N_{Ind}	$N_{females}$	N_{males}	**Mean (SD)**	V_P **(SE)**	V_A **(SE)**	V_M **(SE)**	V_{YBirth} **(SE)**	V_R **(SE)**
Lifetime reproductive success	447	301	146	3.69 (2.37)	0.154 (2.45×10^{-5})	0.007 (2.90×10^{-5})	0.006 (2.72×10^{-5})	0.037 (6.59×10^{-5})	0.104 (7.24×10^{-5})

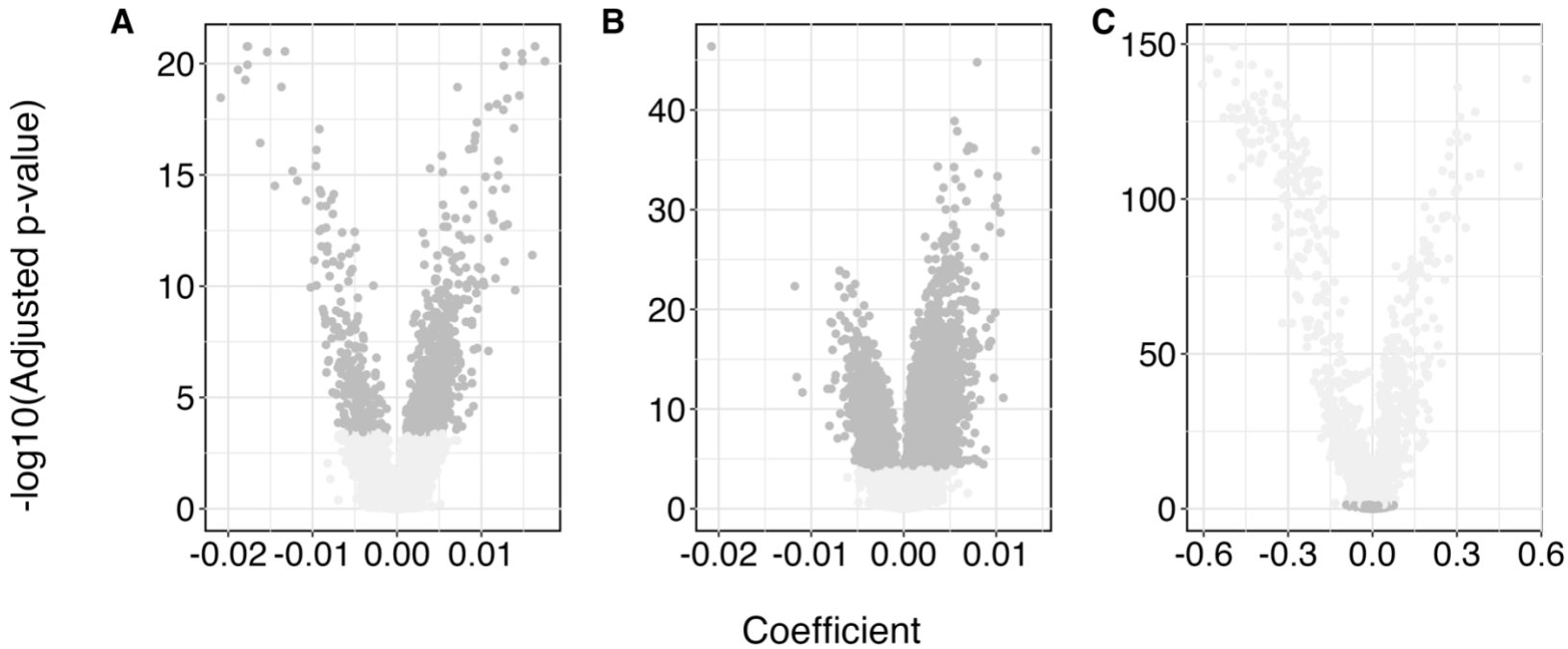

Extended Data Figure 1. Volcano plots showing sites included in clock (dark grey) and excluded from the clock (light grey) because the coefficients from blood (a) and skin (b) samples were either not significantly associated with age, or both skin and blood samples were associated with sex (c).

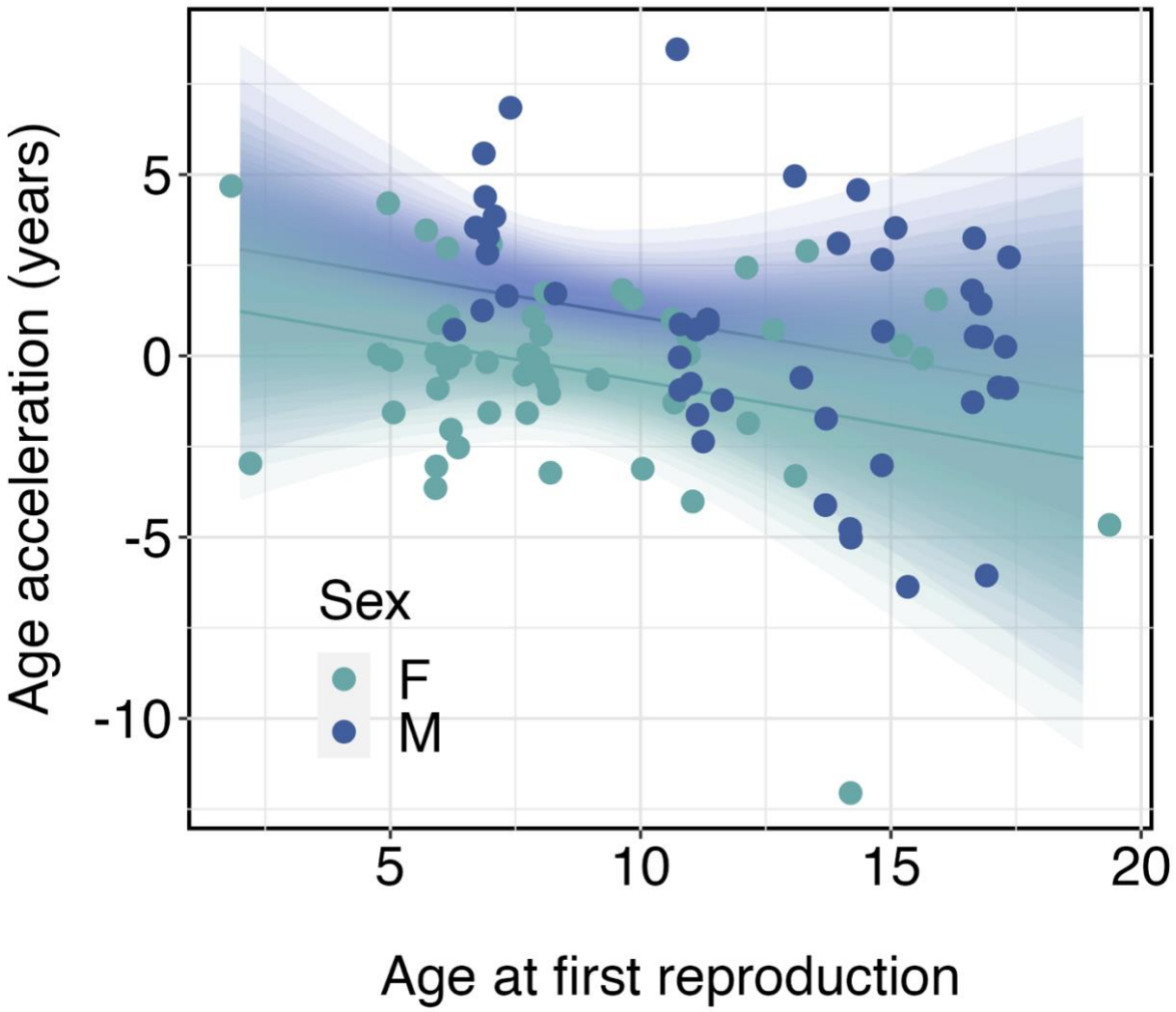

Extended Data Figure 2. Effect of age at first reproduction on epigenetic age acceleration for n = 100 male (blue) and female (seafoam) western Hudson Bay polar bears (Ursus maritimus). Points represent measurements of age acceleration from individuals sampled between 1988 and 2016, and the line and ribbon represent the mean and 95% percentile interval around the posterior distribution estimated using a Bayesian generalized linear model.

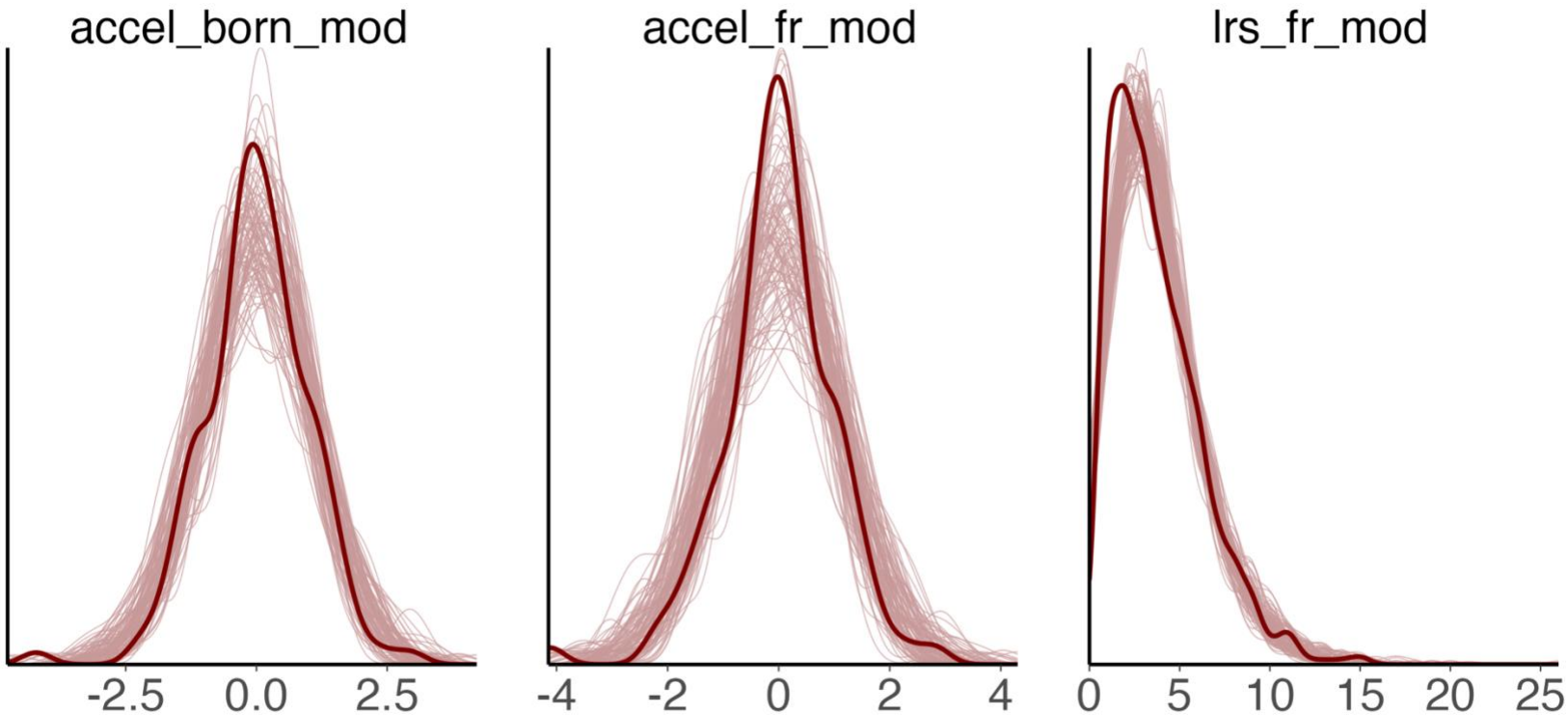

Extended Data Figure 3. Plots showing posterior predictive checks for Bayesian generalized linear models. Draws from the posterior predictive distribution (thin lines) are compared against the observed data (thick lines). Models include change in age acceleration with birth year (accel_born_mod), change in age acceleration with age at first reproduction (accel_fr_mod), and change in lifetime reproductive success with age at first reproduction (lrs_fr_mod).

References

1. Bradshaw, W. E. & Holzapfel, C. M. Evolutionary response to rapid climate change. *Science* **312**, 1477–1478 (2006).
2. Rantanen, M. *et al.* The Arctic has warmed nearly four times faster than the globe since 1979. *Commun Earth Environ* **3**, 168 (2022).
3. Scarpato, R. *et al.* Role of oxidative stress, genome damage and DNA methylation as determinants of pathological conditions in the newborn: an overview from conception to early neonatal stage. *Mutation Research/Reviews in Mutation Research* **783**, 108295 (2020).
4. Lu, A. T. *et al.* DNA methylation GrimAge strongly predicts lifespan and healthspan. *Aging* **11**, 303–327 (2019).
5. Trisos, C. H., Merow, C. & Pigot, A. L. The projected timing of abrupt ecological disruption from climate change. *Nature* **580**, 496–501 (2020).
6. Hoffmann, A. A. & Sgrò, C. M. Climate change and evolutionary adaptation. *Nature* **470**, 479–485 (2011).
7. Antão, L. H. *et al.* Climate change reshuffles northern species within their niches. *Nat. Clim. Chang.* **12**, 587–592 (2022).
8. Charmantier, A. *et al.* Adaptive phenotypic plasticity in response to climate change in a wild bird population. *Science* **320**, 800–803 (2008).
9. Spooner, F. E. B., Pearson, R. G. & Freeman, R. Rapid warming is associated with population decline among terrestrial birds and mammals globally. *Global Change Biology* **24**, 4521–4531 (2018).

10. Diffenbaugh, N. S. & Barnes, E. A. Data-driven predictions of the time remaining until critical global warming thresholds are reached. *Proc. Natl. Acad. Sci. U.S.A.* **120**, e2207183120 (2023).
11. United Nations Environment Programme. *Emissions Gap Report 2023: Broken Record – Temperatures hit new highs, yet world fails to cut emissions (again)*. https://wedocs.unep.org/20.500.11822/43922 (2023) doi:10.59117/20.500.11822/43922.
12. Molnár, P. K. *et al.* Fasting season length sets temporal limits for global polar bear persistence. *Nat. Clim. Chang.* **10**, 732–738 (2020).
13. Galbraith, P. S. & Larouche, P. Sea-surface temperature in Hudson Bay and Hudson Strait in relation to air temperature and ice cover breakup, 1985–2009. *Journal of Marine Systems* **87**, 66–78 (2011).
14. Lunn, N. J. *et al.* Demography of an apex predator at the edge of its range: impacts of changing sea ice on polar bears in Hudson Bay. *Ecol Appl* **26**, 1302–1320 (2016).
15. de La Guardia, C. L., Myers, P., Derocher, A., Lunn, N. & Terwisscha Van Scheltinga, A. Sea ice cycle in western Hudson Bay, Canada, from a polar bear perspective. *Mar. Ecol. Prog. Ser.* **564**, 225–233 (2017).
16. Atkinson, S. N. *et al. 2021 aerial survey of the Western Hudson Bay polar bear subpopulation*. 1–89 (2021).
17. Boonstra, R. *et al.* The stress of Arctic warming on polar bears. *Global Change Biology* **26**, 4197–4214 (2020).
18. Regehr, E. V., Lunn, N. J., Amstrup, S. C. & Stirling, I. Effects of earlier sea ice breakup on survival and population size of polar bears in western Hudson Bay. *Journal of Wildlife Management* **71**, 2673–2683 (2007).

318 19. Stirling, I. & Derocher, A. E. Effects of climate warming on polar bears: a review of the
319 evidence. *Glob Change Biol* **18**, 2694–2706 (2012).
320 20. Pilfold, N. W. *et al.* Mass loss rates of fasting polar bears. *Physiological and Biochemical*
321 *Zoology* **89**, 377–388 (2016).
322 21. Lone, K. *et al.* Aquatic behaviour of polar bears (Ursus maritimus) in an increasingly ice-free
323 Arctic. *Sci Rep* **8**, 9677 (2018).
324 22. Selye, H. *The stress of life*. (McGraw-Hill, 1976).
325 23. Jones, M. J., Goodman, S. J. & Kobor, M. S. DNA methylation and healthy human aging.
326 *Aging Cell* **14**, 924–932 (2015).
327 24. Bateson, M. Cumulative stress in research animals: Telomere attrition as a biomarker in a
328 welfare context? *BioEssays* **38**, 201–212 (2016).
329 25. Levine, M. E. *et al.* An epigenetic biomarker of aging for lifespan and healthspan. 19.
330 26. Oblak, L., van der Zaag, J., Higgins-Chen, A. T., Levine, M. E. & Boks, M. P. A systematic
331 review of biological, social and environmental factors associated with epigenetic clock
332 acceleration. *Ageing Research Reviews* **69**, 101348 (2021).
333 27. Jones, P. A. Functions of DNA methylation: islands, start sites, gene bodies and beyond. *Nat*
334 *Rev Genet* **13**, 484–492 (2012).
335 28. Horvath, S. DNA methylation age of human tissues and cell types. *Genome Biology* **14**, R115
336 (2013).
337 29. Stubbs, T. M. *et al.* Multi-tissue DNA methylation age predictor in mouse. *Genome Biol* **18**,
338 68 (2017).
339 30. Lu, A. T. *et al.* Universal DNA methylation age across mammalian tissues. *Nat Aging* (2023)
340 doi:10.1038/s43587-023-00462-6.

31. Parsons, K. M. *et al.* DNA methylation-based biomarkers for ageing long-lived cetaceans. *Molecular Ecology Resources* 1755–0998.13791 (2023) doi:10.1111/1755-0998.13791.
32. Robeck, T. R. *et al.* Multi-tissue DNA methylation aging clocks for sea lions, walruses and seals. *Commun Biol* **6**, 359 (2023).
33. Horvath, S. *et al.* DNA methylation clocks for dogs and humans. *Proc. Natl. Acad. Sci. U.S.A.* **119**, e2120887119 (2022).
34. Wilkinson, G. S. *et al.* DNA methylation predicts age and provides insight into exceptional longevity of bats. *Nat Commun* **12**, 1615 (2021).
35. Prado, N. A. *et al.* Epigenetic clock and methylation studies in elephants. *Aging Cell* **20**, (2021).
36. Le Clercq, L., Kotzé, A., Grobler, J. P. & Dalton, D. L. Biological clocks as age estimation markers in animals: a systematic review and meta-analysis. *Biological Reviews* brv.12992 (2023) doi:10.1111/brv.12992.
37. Marioni, R. E. *et al.* DNA methylation age of blood predicts all-cause mortality in later life. *Genome Biol* **16**, 25 (2015).
38. Arneson, A. *et al.* A mammalian methylation array for profiling methylation levels at conserved sequences. *Nat Commun* **13**, 783 (2022).
39. Tacutu, R. *et al.* Human Ageing Genomic Resources: new and updated databases. *Nucleic Acids Research* **46**, D1083–D1090 (2018).
40. Hostetter, N. J., Lunn, N. J., Richardson, E. S., Regehr, E. V. & Converse, S. J. Age-structured Jolly-Seber model expands inference and improves parameter estimation from capture-recapture data. *PLoS ONE* **16**, e0252748 (2021).

41. Kirkwood, T. B. L. & Rose, M. R. Evolution of senescence: late survival sacrificed for reproduction. *Phil. Trans. R. Soc. Lond. B* **332**, 15–24 (1991).

42. Stearns, S. C. *The evolution of life histories*. (Oxford University Press, 1992).

43. Malenfant, R. M. *et al.* Evidence of adoption, monozygotic twinning, and low inbreeding rates in a large genetic pedigree of polar bears. *Polar Biol* **39**, 1455–1465 (2016).

44. Bonnet, T. *et al.* Genetic variance in fitness indicates rapid contemporary adaptive evolution in wild animals. *Science* **376**, 1012–1016 (2022).

45. Wilson, A. J. *et al.* An ecologist's guide to the animal model. *Journal of Animal Ecology* **79**, 13–26 (2010).

46. Forester, B. R., Beever, E. A., Darst, C., Szymanski, J. & Funk, W. C. Linking evolutionary potential to extinction risk: applications and future directions. *Frontiers in Ecol & Environ* **20**, 507–515 (2022).

47. Pigot, A. L., Merow, C., Wilson, A. & Trisos, C. H. Abrupt expansion of climate change risks for species globally. *Nature Ecology & Evolution* **7**, 1060–1071 (2023).

48. Murali, G., Iwamura, T., Meiri, S. & Roll, U. Future temperature extremes threaten land vertebrates. *Nature* **615**, 461–467 (2023).

Methods

Summary

We studied biological aging, fitness, and the capacity for adaptation in the western Hudson Bay polar bear (*Ursus maritimus*) population. Using a pedigree previously constructed for the population, we estimated age at first reproduction and lifetime reproductive success. We measured biological aging by first building an epigenetic clock for polar bears, then using it to gauge the rate at which the cells of individual bears from the population aged epigenetically relative to their chronological age. Using Bayesian generalized linear models, we tested for an increase in the rate of epigenetic aging over time, a relationship between age at first reproduction and the rate of epigenetic aging, and changes in lifetime reproductive success with age at first reproduction over time. Finally, we used an animal model, a type of mixed-effects model that estimates the additive genetic variance of traits like lifetime reproductive success[1], to estimate western Hudson Bay polar bears' capacity for adaptation.

Field data collection

Since 1966, polar bears have been captured in northeastern Manitoba near Churchill, Canada as part of a long-term study[2]. Bears are chemically immobilized, sexed, and fitted with unique ear tags and tattoos on the upper lip for later identification in case of recaptures. Skin samples are extracted either from pinna tissue remaining after ear-tagging or using a biopsy punch of superficial rump fat[2]. Blood samples are drawn from femoral blood into a sterile Vacutainer and stored at -80° C[2]. All capture and handling protocols are approved annually by Environment and Climate Change Canada's Prairie and Northern Region Animal Care Committee and wildlife research permits are issued by the Province of Manitoba and by Parks Canada. A standardized

402 sampling program was initiated in 1980 and continues today, with the exclusion of 1985 and
403 1986. As part of this program, adult females and their cubs-of-the-year are sampled in February
404 and March. Chronological age is either derived from known years of birth for cubs-of-the year or
405 based on cementum annulus deposition from an extracted vestigial premolar tooth for bears first
406 captured as adults[3].

407 **Estimating life history traits**

408 We estimated polar bear ages at first reproduction and lifetime reproductive success using
409 previously established pedigree relationships. The western Hudson Bay polar bear population
410 pedigree contains 4,634 polar bears (443 sires, 923 dams, and 1,130 founders, i.e., individuals of
411 unknown parentage) from over six generations sampled between 1966 and 2019. Field sampling
412 data from females and cubs-of-the-year provided offspring-dam associations. Additional linkage
413 information came from parentage analyses using multi-locus microsatellites to genotype
414 individuals[2]. We removed three individuals whose sex classifications were inconsistent with
415 parentage data. These individuals were classified either as male dams or female sires. Additional
416 information about the pedigree construction, capture, handling, and sampling protocols for the
417 Western Hudson Bay subpopulation is described in more detail in[2]. We used the pedigree to
418 estimate lifetime reproductive success and age at first reproduction for all individuals that were
419 confirmed parents of at least one other bear in the pedigree. We defined lifetime reproductive
420 success as the total number of other bears in the pedigree for which an individual was a
421 confirmed parent. We defined age at first reproduction as the age of the individual when its first
422 known offspring was born. In our analyses considering age at first reproduction and lifetime
423 reproductive success, we removed individuals with potentially biased data, using only data from
424 individuals born between 1980 and 2000 (n = 628 bears). Sampling between 1966–1979 was less

425 consistent than post-1980 sampling. By 2019 bears born after 2000 would not have reached 20
426 years, or the approximate age of senescence for western Hudson Bay polar bears[4], which might
427 have resulted in artificially low estimates of lifetime reproductive success. While we expected
428 some error in the absolute ages at first reproduction and lifetime reproductive success because of
429 gaps in the pedigree, we assumed relative comparisons among individuals were unbiased
430 between 1980 and 2000.

431 **Building the epigenetic clock for polar bears**

432 Epigenetic clocks predict chronological ages based on methylation of CpG dinucleotides, where
433 a cytosine is followed by a guanine[5]. Many CpGs change with chronological age. The Illumina
434 HorvathMammalMethylChip40 array (Illumina Inc., San Diego, CA, USA; hereafter mammalian
435 array) was designed to analyze methylation at CpG sequences highly conserved across all
436 mammalian species, measuring a total of 37,449 unique sequences per sample at a single
437 nucleotide resolution. The high-throughput array can process 96 samples simultaneously, making
438 this approach useful for aging samples from long-term ecological projects that store many
439 samples over multiple years.

440 To build our epigenetic clock, we randomly selected from 6,135 blood and skin samples
441 collected from western Hudson Bay polar bears aged 0–30 over the sampling period. We
442 stratified sampling based on individual age, tissue type, sex, and year of sample collection. We
443 ensured at least some samples came from bears that were sampled more than once over their
444 lifetimes to test for consistency in individual aging rates over time (Figure 2). To test for
445 consistency in DNA methylation rates between tissues, we also included several samples with
446 blood and skin collected at the same time. Our final 288 samples included 150 female and 138
447 male samples from 223 unique individuals, collected between 1988–2018, of which 111 were

448 blood and 177 were skin. Five individuals were sampled either 4, 9, 10, 11, or 13 times
449 throughout their lives and another 25 individuals were sampled twice. All sample details,
450 including ages, sexes, and dates of sampling are available in Supplementary Data File 1.

451 We isolated genomic DNA from blood and skin samples using the Qiagen DNeasy Blood
452 and Tissue Kit 250 (Qiagen, Hilden, Germany). We dissected approximately 25 mg of frozen
453 skin samples on a pre-chilled plate placed on dry ice to prevent thawing of the entire tissue. We
454 then cut the skin tissue into smaller pieces, placed it in 1.5 mL microcentrifuge tubes, and
455 digested it overnight in Buffer ATL (Qiagen) and Proteinase K (Qiagen) solution at 56 °C. We
456 also digested 50 µL volumes of blood samples in Proteinase K (Qiagen) and PBS (pH 7.4, 1X,
457 Gibco) solution at 56 °C for 10 minutes. After tissue digestion, we extracted genomic DNA from
458 the samples as per manufacturer's protocol (Document #HB-0540-002, Version #04/2016) and
459 eluted the samples in two 100 µL volumes of elution buffer (Qiagen) consecutively to increase
460 yield. We measured the concentration of gDNA using the NanoDrop2000 spectrophotometer
461 (Thermo Scientific, Wilmington, USA). Next, we treated 750 ng of each genomic DNA sample
462 with sodium bisulfite using the EZ-96 DNA Methylation-Gold Kit (shallow-well format) (Zymo
463 Research, CA, USA) as per manufacturer's protocol (Document #D5007, Version #2.1.6). We
464 eluted the bisulfite converted DNA in 12 µL of elution buffer (Zymo Research), after which we
465 amplified 4 µL from each sample to be hybridized onto the mammalian array following the
466 Infinium HD Methylation Assay protocol (Document #15019519, Version #07).

467 We measured DNA methylation by imaging the hybridized chips on the same day they
468 were stained using the iScan instrument (Illumina Inc., San Diego, CA, USA). We normalized
469 the raw intensity data or IDAT files from the chip scans using the recommended pipeline in the
470 *minfi* package in R (Aryee et al. 2014). Normalized intensity data, hereafter **β** values, quantify

471 the degree of methylation at each of the 37,449 sites on the mammal chip with a value between 0
472 for no methylation and 1 for 100% methylation at each site.

473 The design of the mammalian array, while appropriate for any mammal species, presents
474 some practical challenges in terms of accurately quantifying methylation in the genomes of
475 specific species. First, all 37,449 CpG sequences on the array might not bind to the genomes of
476 all species because of species-specific CpG differences. Alternatively, a single sequence might
477 bind multiple times in the genome of a given species because probes were designed with up to
478 three degenerate bases to facilitate matching in case of cross-species mutations[6]. Sequences that
479 bind multiple times can confound methylation signals coming from multiple sites at once[6].
480 Methylation can also vary by sex if CpG sequences are located on the sex chromosomes[7], a
481 particularly important concern for the mammalian array because of species-specific locations of
482 CpG sequences on chromosomes.

483 To minimize potential confounds from sex-specific site methylation and non-binding or
484 multiple binding probes, we narrowed our probe search space before building our clock. First,
485 we aligned the CpG sequences on the mammalian array to a reference polar bear genome (NCBI
486 Genome assembly ASM1731132v1
487 https://www.ncbi.nlm.nih.gov/datasets/genome/GCF_017311325.1/) using the *QuasR* package
488 v1.40.1[8] in R v4.3.1[9]. We selected only the 33,674 sites that bound uniquely. We also limited our
489 search space with an epigenome-wide association study (EWAS), a technique which correlates
490 phenotypic traits with epigenetic modifications including DNA methylation. We used our EWAS
491 to isolate sites with methylation patterns related to age but not different between sexes. We fit
492 three linear models with site-specific CpG methylation proportions as the response and
493 combinations of age and sex as predictors using the *limma* package v3.56.2 in R[10]. In the first

494 model we included tested the effects of sex on methylation while controlling for ages and tissue
495 types of samples. We also fit two models including only either blood or skin samples to isolate
496 the effects of age on the proportion of methylation in either tissue. We excluded 3,740 CpG
497 sequences significantly associated with sex ($p < 0.05$) and 29,573 that were not sufficiently
498 associated with age ($p > 10e^{-6}$). We erroneously excluded another 23 (0.007%) CpG sites. We
499 used a final 3,328 of the 37,449 CpG sites on the HorvathMammalMethylChip40 array in the
500 model we used to build our clock (Supplementary Data File 2).

501 We fit our DNAm clock using a training set of 144 samples (Supplementary Data File 1)
502 from our original 288 samples. We first screened unreliable samples from the training data by
503 predicting epigenetic ages in our samples using the universal clock for mammals[11]. We screened
504 10 samples from the training data either because their scans failed on the iScan or the normalized
505 **β** values did not pass quality control tests. Because we included bears from a single population,
506 we were also concerned that potential relatedness between individuals used to build the clock
507 might bias its predictions. We used the *GeneAlEx 6.5* software[12] to assess relatedness between
508 individuals and screened any individuals from the training data with a relatedness index > 0.25.
509 We also screened any individuals with repeat samples from the training data. We used the
510 training data to fit the **β** ~ age clock model using the cv.glmnet function in the *glmnet* package
511 v4.1-8 in R[13], setting **α** = 0.5 to combine the benefits of both ridge and lasso regression. This
512 compromise reduces the variance in age predictions at the cost of some bias. We used 10-fold
513 cross validation select the optimal regularization parameter. We validated our clock by using it to
514 predict the chronological ages of all remaining samples (n = 134; Supplementary Data File 1).
515 CpG sites and **β** values are available in Supplementary Data File 3.

516 **Statistical analysis**

Generalized linear models

We used Bayesian generalized linear models to test for a change in epigenetic age acceleration over time, for a relationship between age acceleration and age at first reproduction, and for a relationship between age at first reproduction and lifetime reproductive success. We fit all models using the *brms* package v2.20.4 in R[14], with 4 chains and 10,000 iterations including 5,000 warmup iterations. For the first two models — age acceleration over time and with age at first reproduction — we specified a gaussian link function and used weakly informative prior slopes with mean 0 and standard deviation 1. We tested for a relationship between birth year and age acceleration using n = 134 bears aged 0–30 born between 1966–2013. We tested for a relationship between age at first reproduction and age acceleration for n = 100 bears with epigenetic age estimates and known offspring. We included an effect for sex in both models to control for differences in age acceleration between male and female bears. We also included random effects in both models to account for individual differences and for multiple measures from individuals. We included n = 628 bears born between 1980–2000 in our model testing the effect of age at first reproduction on lifetime reproductive success. For this model we specified a negative binomial response distribution with a log link function, using weakly informative prior slopes with mean 0 and standard deviation 1. We included an interaction between age at first reproduction and birth year.

Animal model

We used an animal model[1] to estimate the additive genetic variance of lifetime reproductive success for 628 polar bears. We used the pedigree data to create a genetic relatedness matrix. We fit this matrix as the random effect '*animal*' to estimate additive genetic variance (V_A). Phenotypic variance (V_P) is partitioned into additive genetic variance (V_A) and a residual variance

(V_R) component, which is interpreted as the environmental effect. We further partitioned the residual variance by including maternal variance (V_M, or the identity of individual's dam) and cohort variance (V_{YBirth}, or year of birth). We also included sex as a fixed effect in the model. We used a log link function, an inverse-Gamma distribution for the random effect variances, and a wide normal distribution for the prior distribution of fixed effects[15]. We fit the animal model in the package *MCMCglmm* v2.35[16] in R with 1,000,000 iterations and 20,000 warmup iterations. The *MCMCglmm* package allows incomplete pedigrees and uses Bayesian inference and Markov chain Monte Carlo (MCMC) methods.

548 ## References

549 1. Wilson, A. J. *et al.* An ecologist's guide to the animal model. *J. Anim. Ecol.* **79**, 13–26
550 (2010).
551 2. Malenfant, R. M. *et al.* Evidence of adoption, monozygotic twinning, and low inbreeding
552 rates in a large genetic pedigree of polar bears. *Polar Biol.* **39**, 1455–1465 (2016).
553 3. Calvert, W. & Ramsay, M. A. Evaluation of age determination of polar bears by counts of
554 cementum growth layer groups. *Ursus* 449–453 (1998).
555 4. Derocher, A. E., Stirling, I. & Andriashek, D. Pregnancy rates and serum progesterone levels
556 of polar bears in western Hudson Bay. *Can. J. Zool.* **70**, 561–566 (1992).
557 5. Horvath, S. DNA methylation age of human tissues and cell types. *Genome Biol.* **14**, R115
558 (2013).
559 6. Arneson, A. *et al.* A mammalian methylation array for profiling methylation levels at
560 conserved sequences. *Nat. Commun.* **13**, 783 (2022).
561 7. Inkster, A. M., Wong, M. T., Matthews, A. M., Brown, C. J. & Robinson, W. P. Who's afraid
562 of the X? Incorporating the X and Y chromosomes into the analysis of DNA methylation
563 array data. *Epigenetics Chromatin* **16**, 1 (2023).
564 8. Gaidatzis, D., Lerch, A., Hahne, F. & Stadler, M. B. QuasR: quantification and annotation of
565 short reads in R. *Bioinformatics* **31**, 1130–1132 (2015).
566 9. R Core Team. R: A language and environment for statistical computing. (2023).
567 10. Ritchie, M. E. *et al.* limma powers differential expression analyses for RNA-sequencing and
568 microarray studies. *Nucleic Acids Res.* **43**, e47–e47 (2015).
569 11. Lu, A. T. *et al.* Universal DNA methylation age across mammalian tissues. *Nat. Aging* (2023)
570 doi:10.1038/s43587-023-00462-6.

12. Peakall, R. & Smouse, P. E. GenAlEx 6.5: genetic analysis in Excel. Population genetic software for teaching and research—an update. *Bioinformatics* **28**, 2537–2539 (2012).
13. Friedman, J., Hastie, T. & Tibshirani, R. Regularization paths for generalized linear models via coordinate descent. *J. Stat. Softw.* **33**, (2010).
14. Bürkner, P.-C. brms: An R package for Bayesian multilevel models using Stan. *J. Stat. Softw.* **80**, (2017).
15. De Villemereuil, P. Quantitative genetic methods depending on the nature of the phenotypic trait. *Ann. N. Y. Acad. Sci.* **1422**, 29–47 (2018).
16. Hadfield, J. D. MCMC Methods for multi-response generalized linear mixed models: The **MCMCglmm** *R* Package. *J. Stat. Softw.* **33**, (2010).